



26 use and land cover map were generated by using Landsat-8 image acquired on August 10th 2015
27 was classified to distinguish mainly the alluvial deposit from the mountainous rock. The study
28 reveals that hydrological evaluation using ASTER GDEM is more precise and applied with
29 compared to other techniques at the watershed scale.

30 **Keywords:** Hydrological characteristics, Morphometric characteristics, Remote Sensing and GIS
31 techniques, Wadi Yalamlam, Watershed management.

32 **1. Introduction**

33 The choice of an optimal interpolation method, for the prediction of soil properties at unsampled
34 locations, is a subject of great importance in agricultural management studies. Several attempts
35 had been made in order to specify the most accurate interpolation technique for the generation of
36 continuous soil attributes surfaces.

37 Most of the soil studies using interpolation techniques include the Inverse Distance Weighted and
38 Kriging methods. The accuracy of these methods has been compared in several studies. Gotway et
39 al. (1996) found that the IDW method generated more accurate results for mapping soil organic
40 matter and soil NO₃ levels. Wollenhaupt et al. (1994) compared these two interpolation techniques
41 and concluded that IDW was more accurate for mapping P and K levels of soil. Mueller et al.
42 (2004) observed that for the optimal parameters of the method, the accuracy of IDW interpolation
43 generally equaled or exceeded the accuracy of kriging at each scale of measurement. On the other
44 hand, other researchers observed Kriging to be more accurate for the interpolation of soil attributes.
45 Leenaers et al. (1990) found Kriging interpolation method the most accurate in comparison to
46 IDW, for mapping soil Zn content.



47 Other studies compared Kriging IDW and Radial Basis Functions interpolation techniques in soil
48 science. Schloeder et al. (2001) observed that Ordinary kriging and inverse-distance weighting
49 were similarly accurate and effective methods, while thin-plate smoothing spline with tensions
50 was not. Weller et al. (2007) resolved that not only the predications for kriging were not satisfied
51 the kriging method, but also was as good as any other radial base function interpolation.

52 Since the early decades of the century, spatial variability of soil properties has been widely studied
53 in order to understand the behavior of soils for agricultural purposes. Knowledge, of spatial
54 variability and relationships among soil properties, is important for the generation of soil maps for
55 reasons of land management.

56 Hydrological parameters are essential for adequate water resources management plans.
57 Morphometric characteristics aim to investigate the watershed delineation, site selection in water
58 recharge and discharge, run off modelling and other geomorphological studies (Sreedevi et al.,
59 2013; Elhag, 2015). GIS helps a wide variety of basin characterization and evaluation applications
60 under different terrain conditions (Pankaj and Kumar, 2009; Magesh et al., 2011).

61 Digital Elevation Model (DEM), such as ASTER GDEM (USGS, USA) is the keystone
62 involvement in various extractions of Geo hydrological parameters of the watershed. Several
63 parameters including slope, aspect, stream network, and upstream flow areas can be conducted
64 from the DEM characterization (Grohmann et al., 2007; Elhag, 2015). Reliable results of
65 implementing Remote sensing and GIS based morphometric evaluation using ASTER GDEM data
66 have been reported in numerous scholarly work of watershed characterization (Farr and Kobrick,
67 2000; Panhalkar, 2014; Elhag, 2015). Author's refers that ASTEDR GDEM is more useful and



68 very accurate tool for the watershed delineation and morphometric evaluation for the watershed
69 management.

70 The conducted results of the current study discuss that the analysis of methodical information and
71 further hydrological and morphometric investigation can find out satisfactory alternative strategies
72 for adequate rainwater harvesting based on observed calculations in the designated study
73 watershed. The main aim of the present study is to identify and investigate various drainage
74 attributes to geometrical evaluation of Yalamlam basin for the sustainable rainwater harvesting
75 management and conservation of water resources.

76 **2. Materials and Methods**

77 **2.1. Study Area**

78 Wadi Yalamlam basin is located about 125 km southeast of Jeddah city and is bounded by latitudes
79 $20^{\circ} 26'$ and $21^{\circ} 8'N$ and longitudes $39^{\circ} 45'$ and $40^{\circ} 29'E$ (Figure 1). Wadi Yalamlam basin drained
80 large catchment area of about 180,000 hr. The basin boundary of the lower part is enlarged to
81 include nearly all the flat area in the downstream part. Wadi Yalamlam basin is initiated from high
82 elevation Hijaz escarpment with mean annual rainfall of about 140 mm. The basin elevations are
83 greatly varies from upstream and downstream parts and range between 2850 m and 25 m (a.s.l.)
84 respectively. The main course of Wadi Yalamlam is crosscut the highly fractured granitoids,
85 gabbroic and metamorphic rocks until the coastal plain of the Red Sea. The upper and middle parts
86 of Wadi Yalamlam basin are covered by intense natural vegetation. The lower part is covered
87 mainly by Quaternary deposits and sand dunes with small-scattered highly altered granitoids and
88 metamorphosed basaltic hills. Several basic dykes are recorded in the lower part of Wadi
89 Yalamlam basin. The thickness of Quaternary wadi deposits increased in the lower part (Elhag and



90 Bahrawi 2017). Regional groundwater flow drains toward the south and southwest following the
91 general trend of the main wadi channel. The gradient of the water table varies from one area to
92 another according to the variations in the pumping rates and hydraulic properties of the aquifer. It
93 has an average value of about 0.011. The high pressure of the subtropical zone in addition to local
94 topography affects climate in Yalamlam basin. Both regional and local circulations have a
95 dominant influence on the climate of the region. From the temperature records in the Red Sea coast
96 stations, the mean monthly maximum temperature is 38°C and the mean monthly minimum
97 temperature is 20°C. The highest recorded temperature in July is 49°C and the lowest in January is
98 12°C. The maximum mean monthly evaporation value is around 500 mm in summer, where in
99 winter it is about 200 mm (Elhag, 2016)



100

101 **Figure 1. Location of the study area (Elhag 2016).**

102 **2.2. Soil sampling**

103 Map accuracy and quality depends on the sampling method to be used, scale, analytical laboratory
104 errors and prediction errors. Sampling approaches depend on the objectives of the study that are
105 highly correlated to scale. Random Stratified Sampling was the adopted sampling design, the



106 landscape is divided into smaller areas, named strata, and afterwards 150 random samples are taken
107 from the designated study area.

108 **2.3. Physical and Chemical soil analysis**

109 Each individual sample was analyzed separately and each measurement was repeated three times
110 for the same extract. Thus, the final values of the measured attributes are represented by the mean
111 value of nine measurements. Soil samples were analyzed in order to estimate physical analysis
112 (clay, silt and sand) and chemical analyses (pH, Calcium Carbonate, Electric Conductivity,
113 Minerals and Organic Content) including all samples.

114 For standard particle size measurement, the soil fraction that passes a 2-mm sieve is considered.
115 Laboratory procedures normally estimate percentage of sand (0.05 - 2.0 mm), silt (0.002 - 0.05
116 mm), and clay (<0.002 mm) fractions in soils. Soil particles are usually cemented together by
117 organic matter; this has to be removed by H₂O₂ treatment. However, if substantial amounts of
118 CaCO₃ are present, actual percentages of sand, silt or clay can only be determined by prior
119 dissolution of the CaCO₃.

120 The chemical procedures presented here are extensive, though by no means exhaustive. For any
121 given element, there are several procedures or variations of procedures can be found in the
122 literature (Walsh and Beaton, 1973; Westerman, 1990). Procedure for determining soil pH in a 1:1
123 (soil: water) suspension was after McLean (1982). The methodology of EC measurement is given
124 in USDA Handbook 60 (Richards, 1954). Active CaCO₃ is usually related to total CaCO₃ equivalent,
125 being about 50% or so of the total value. Total CaCO₃, is currently estimated after Drouineau (1942).

126

127 **2.4. Interpolation techniques**



128 Geostatistics interpolation is based on the assumption that all values of a variable that is measured
129 are the result of a random process. The phrase "random process" does not indicate that all events
130 are independent. More specifically Geostatistics is based on random processes with dependence,
131 otherwise called autocorrelation, and relies on some notion of replication. Repeated observations
132 in nature can result in understanding the variation and uncertainty of natural phenomena, and
133 furthermore in estimating their sequence in space and time. Three interpolation techniques were
134 used for the generation of the prediction maps (interpolation). Inverse Distance Weighted (IDW),
135 Radial Basis Function (RBF) and Ordinary Kriging (OK) method were compared according to the
136 accuracy of the results.

137 Spatial distribution equation (Weibel, 1997):

$$138 \quad Y_{(k)} = \frac{1}{2 \times n(k)} \times \sum_{i=1}^{n(k)} [Z(x_i) - Z(x_{i+k})]^2$$

139 Where: $n(k)$ - number of pairs of observation; $Z(x_i)$ - soil property measured in point x , and in point
140 $x + k$.

141 Interpolation equation (Stoer and Bulirsch, 1980)

$$142 \quad Z(x_0) = \sum_{i=1}^n \lambda_i \times Z(x_i)$$

143 Where: $Z(x_0)$ - interpolated value of variable Z at location x_0 , $Z(x_i)$ - values measured at location
144 x_i ; λ_i ; - weighed coefficients calculated based on the semivariogram.

145 Trend and random error equation (Johnson and Riess, 1982)

$$146 \quad Z(S) = \mu(S) + \varepsilon(S)$$

147 The symbol s stands for the location of the prediction location. $Z(S)$ is the variable you are
148 predicting (total extractable heavy metal concentration). $\mu(S)$ is the deterministic trend. $\varepsilon(S)$ is the
149 spatially-autocorrelated random error.

150 **2.5. Morphometric parameters**



151 Based on the foundation scholarly work of Horton (1945), Schumm (1963), Strahler (1964) and
152 others, several morphometric parameters were performed and computed utilizing ASTER GDEM
153 under GIS environment. Consequently, watershed delineation, stream network identification,
154 drainage frequency, drainage density, shape, elongation ratio, circularity ratio and form factor were
155 computed and evaluated using 30m spatial resolution of ASTER GDEM. The methodologies
156 adopted for the evaluation and computation of morphometric features are given in Table 1.

157 **2.6. Supervised classification**

158 Remote sensing data was obtained from Landsat Operational Land Imager (OLI-8) which is
159 acquired on June 10th, 2013. Typical atmospheric and radiometric corrections and spatial
160 resolution enhancement were implemented for each band individually. Furthermore, supervised
161 classification was implemented using Support Vector Machine (SVM) classifier for better
162 classification results (Psilovikos and Elhag, 2013). The final step in the digital image analysis is
163 the evaluation of the accuracy of the computer derived classification results. These results are often
164 expressed in tabular form, known as a confusion matrix (Elhag et al., 2013). The SVM classifier
165 is implemented as:

$$166 \quad K(x_i, x_j) = \tanh(gx_i^T x_j + r)$$

167 Where:

168 g is the gamma term in the kernel function for all kernel types except linear

169 r is the bias term in the kernel function for the polynomial and sigmoid kernels.

170

171 **Table 1. Summary of the implemented morphometric features:**

Item	Morphometric feature	Equation	Citation
1	Stream length (L_u)	Length of the stream	Horton (1945)
2	Stream length ratio (R_i)	$R_i = L_u / (L_u + 1)$	Horton (1945)



3	Form factor (F_f)	$F_f = A/L^2$	Horton (1945)
4	Drainage frequency (F_d)	$F_d = N_u / A$	Horton (1945)
5	Drainage density (D_d)	$D_d = L_u / A$	Horton (1945)
6	Drainage texture (T)	$T = D_d * F_d$	Smith (1950)
7	Bifurcation ratio (R_b)	$(R_b) = N_u / (N_u + 1)$	Schumm (1956)
8	Elongation ratio (R_e)	$R_e = D/L$	Schumm (1956)
9	Mean bifurcation ratio (R_{bm})	R_{bm} = average of bifurcation ratios	Strahler (1957)
10	Relief (R)	$R = H-h$	Hadley & Schumm (1961)
11	Relief ratio (R_r)	$R_r = R/L$	Schumm (1963)
12	Stream order (S_r)	Hierarchical rank	Strahler (1964)
13	Stream no	Order wise no of streams	Strahler (1964)
14	Mean stream length (L_{sm})	$L_{sm} = L_u / N_u$	Strahler (1964)
15	Circularity ratio (R_c)	$R_c = 4\pi A / P^2$	Strahler (1964)

Where

A =Area of the basin (km²)

D_d =Drainage density

F_f =Form factor

F_d =Stream frequency

L =Basin length (km)

L_{sm} = Mean stream length

L_{u+1} = The total stream length of its next higher order u

L_u = The total stream length of order u

N_{u+1} = Number of stream segments of the next higher order

N_u = The no. of stream segments of order u

P =Perimeter (km)

R_b = Bifurcation Ratio

R_c =Circularity ratio

R_e =Elongation ratio

RL =Stream Length Ratio

T =Drainage texture

π =3.14

172

173 3. Results and Discussion

174 Quantitative evaluation of the watershed through the analysis of morphometric parameter can
 175 provide significant information about the hydrological characteristics of rocks, which are exposed
 176 within the basin. The nature of drainage of a basin reveals reliable information about the
 177 permeability of the rocks and the yield of the basin.



178 The ASTER GDEM has been collected with 30 m resolution and the GDEM has been used to
179 generate watershed area, aspects and slope map of the basin. The drainage network of a basin
180 depends on endogenous forces and exogenous forces. Geology and precipitation pattern of the
181 study area. ASTER GDEM was used for preparing aspects, slope map of the basin. Areal, relief
182 and linear aspects of the basin were analyzed under GIS environment. Currently a geospatial
183 technology has been given more precise and accurate information through the evolution of
184 morphometric parameter for the assessment of drainage watershed. GIS technology and satellite
185 data have been used to formulate data on spatial deviations in drainage attributes. Therefore,
186 drainage parameter provides a significant insight into hydrological characteristics, which is more
187 important to develop the watershed management strategies (YanYun et al., 2014).

188 Evaluation of drainage characteristics and other morphometric parameter of Yalamlam basin has
189 been undertaken to calculate the parameter and built topology of the basin. Different type of Aerial
190 and linear aspects and their characteristics has been calculated, these aspects are, basin area (A),
191 basin length (L), basin perimeter (P), bifurcation ratio (Rb), elongation ratio (Re), circularity ratio
192 (Rc), drainage frequency (Fd) and drainage density (Dd) etc.

193 **3.1. Stream order (S_o) and stream no:**

194 The lower Yalamlam basin encompasses through the basin mega fan, which is formed by ancient
195 and modern radial drainage pattern in the designated study area. The channel of this area is
196 characterized by higher sinuous, decreased widths and lesser discharge capacity as a numerous
197 traverse Paleo alluvial channels (Bahrawi et al., 2016). Therefore, the stream ordering of the study
198 area has been ranked based on Strahler (1964) method and demonstrated in Table 2.

199 **Table 2. Stream network order based on Strahler method.**



Strahler	Cnt_Strahler	Rb	Nu-r	Rb * Nu-r	Sum_Length
1	598				872.847
2	135	4.42963	733	3246.919	452.488
3	22	6.13636	157	963.409	237.306
4	6	3.66667	28	102.667	112.047
5	2	3.00000	8	24.000	54.635
6	1	2.00000	3	6.000	58.259
Sum	764	19.232659932	929	4342.99427609428	1787.582302
Mean		3.847		4.675	

200

201 **3.2. Bifurcation ratio:**

202 The bifurcation ratio was calculated by the no of streams of an order to the no of the streams of
 203 the next higher order. The values vary from 2.0 to 4.42 of the Yalamlam streams basin, which is
 204 also signified the maximum structural influences (Strahlar, 1964). After the calculation of
 205 bifurcation ratio, calculate the average value which is the mean bifurcation ratio is 3.84 of the
 206 basins. The value also indicates that the drainage pattern has been affected by structural
 207 disturbances within the basin. The obtained no of bifurcation ratio varies from one order to another
 208 order. Such variation is interpreted as irregularities of the lithological and the geological
 209 development within the watershed. The values of bifurcation ratio and mean bifurcation ratio have
 210 been shown in Table 3.

211 **3.4. Drainage texture and drainage density:**

212 Drainage density is an expression of spacing and distribution of channels as proposed by Horton
 213 (1932) that measure the total length of the streams of all orders as calculated with per unit area.
 214 Relative relief and slope gradient of the river basin primarily control the stream density. The stream
 215 density of the watershed has been calculated which is shown in Table 3. The value of drainage



216 density is 0.92 in the study basin. The drainage density has been classified into five kinds of
217 drainage texture as proposed by Smith (1950).

218 The drainage density more than 8 indicates very fine, the value 8-6 is fine, between 6-4 is moderate,
219 the value 4 to 2 is coarse and less than 2 represent very coarser drainage texture. The observer
220 drainage texture is 0.138, signifies the resistant permeable rock with moderate infiltration rate and
221 moderate relief (Bahrawi et al., 2016). The value of the variation of drainage texture depends on
222 different kind of natural factors that is rainfall and other climatic characteristics, rock, soil type,
223 vegetation characteristics, permeability, relief, infiltration capacity within the watershed. The
224 relationship between the hydrological features and the geological structures is estimated to be with
225 a high drainage density caused by the mountainous relief in the basin. The lower value of drainage
226 density reveals that, the region is composed of permeable sub surface material, low relief, dense
227 vegetal cover which results in the increase of more infiltration capacity in the basin. The value of
228 high drainage density indicates mountainous relief, thin vegetation and impermeable sub surface
229 material, highly resistant rock types in the river basin.

230 **3.5. Drainage frequency:**

231 Drainage frequency or stream frequency is calculated by the total no of streams per unit area of all
232 stream orders that proposed by Horton (1932). The correlation value of drainage density and
233 stream frequency is plays positive of the basin, which suggests that the no of streams, population
234 has increases with the increase of drainage density. The observed value of stream, frequency is
235 about of 0.34 for the watershed exhibits the highly positive connection with stream density that
236 has been shown in Table 3.

237 **3.6. Elongation ratio:**



238 The elongation ratio is calculated by the ratio between maximum length of the basin and the
239 diameter of a circle, which fitted in the same basin area, as proposed by Schumm, (1956). The
240 elongation ratio value generally varies between 0.6 and 1.0 where a wide variety of geological
241 condition and climatic characteristics has. According to Strahlar (1964) the values close to 1.0
242 represent the region belongs to very low relief with less structural influences and the value ranges
243 from 0.8 to 0.6 are generally associated with much steep slope and high relief. The values of
244 elongation ratio can be categorized into 3 groups, namely less than 0.7 indicates elongated shape,
245 and 0.8 to 0.9 values represent the oval shape and more than 0.9 values represent the circular shape
246 of the basin. So, the elongated ratio of the study area is 0.14 that suggests that the basin shape is
247 belongs to the much more elongated type (Table 3) of the basin where structural influence is much
248 all over the basin.

249 **3.7. Circularity ratio:**

250 According to Miller (1953) circularity ratio is the ratio between the area of a circle, which fitted
251 in the basin perimeter, and the total basin area. Circularity ratio is much more influenced by
252 geological structure, relief, slope, climate, frequency and length of stream and land use land cover
253 within the basin. The basin circularity ratio is 0.08, which represents that the basin is strongly
254 elongated and belongs to the heterogeneous geological structure and materials. The observed
255 values also signify the high run off capacity and low permeable capacity of subsoil and sub-surface
256 soil along the basin area (Table 3).

257 **3.8. Form factor:**

258 Horton (1932) defines the form factor as the ratio between the square of the basin length and basin
259 area. The values of form factor represent the flow intensity of the study area. Generally, the



260 elongation shape and the values of form factor have a negative relationship that means the smaller
261 value indicates the more elongated shape of the basin. The values should always be not exceeds
262 0.7854, higher value of form factor represent the higher peak flows of a higher period. The
263 observed value of form factor is 0.06 of the Yalamlam watersheds signifies the elongated shape of
264 the basin (Table 3). Therefore, the lower values and elongated shaped basin indicates that the
265 watershed belongs to the flatter peak flow of shorter duration.

266 **Table 3. Wadi Yalamlam morphometric features**

Parameters	Descriptions	Remarks
Basin area (km ²)	1940.3	The basin area is too large
Basin length (km)	60.56	Basin length is very high
Basin perimeter (km)	417	High basin perimeter
Elongation ratio	0.14	Elongated
Form factor	0.06	Elongated shape and flatter peak flow
Circularity ratio	0.08	Strongly elongated and heterogeneous geological structure
Drainage frequency	0.34	Low stream frequency
Drainage density	0.92	Drainage density is considerably high
Drainage texture	0.138	Highly resistant permeable rock with moderate infiltration rate

267

268 **3.9. Relief and relief ratio if the watershed:**

269 Relative relief is the difference between the highest and lowest elevation of the watershed. The
270 relief ratio is the ratio between relative relief and the maximum length of the basin as proposed by
271 Schumm, (1956). It can analyses the steepness of the basin and evaluate the intensity of erosion
272 process of the study area. Here the relief ratio is 4.17, which indicated that most of the designated
273 basin is situated along the mountainous rough slope and much narrower in the lower areas.

274 **3.10. Slope map:**



275 Slope is the ratio between horizontal and vertical surface, of a region, which can be expressed by
276 the percentage and degree. It was found that the most of the area (upper middle part) of Yalamlam
277 watershed comes under steep, very steep and very high steep slopes that indicate the area having
278 a much mountainous topography. The main channel slope of the basin comes under gentle slope
279 (0.042) which designed to flat topography and excellent for the ground water management through
280 favoring for infiltration.

281 **4. Geo hydrological Inferences from Morphometric Evaluation:**

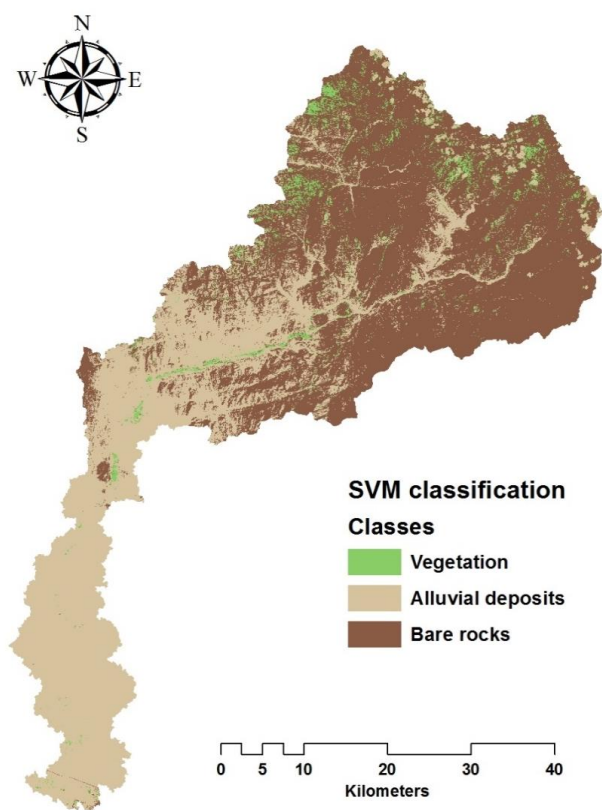
282 The classification of Remote Sensing data was to quantify the area of all alluvial deposits to the
283 bare rock area within the designated study area as illustrated in Figure 2. Table 4 indicates that the
284 area of the alluvial deposits is roughly equal to the bare rock area which means that the watershed
285 is the watershed is likely to be used for rainwater harvesting (Elhag, 2014 and Elhag and Bahrawi
286 2014 a).

287 **Table 4. Wadi Yalamlam land cover classifications**

Land cover category	Area sq. km	Percentage (%)
Vegetation	82.7	4.26
Alluvial deposit	803.3	41.4
Bare rocks	1054.3	54.3
Total	1940.3	100

288

289



290

291 **Figure 2. Supervised classification of Yalamlam basin.**

292 Morphometric evaluation of the Yalamlam basin based on ASTER GDEM with remote sensing
293 and GIS techniques is the most significant method for proper and precise interpretation of
294 hydrological parameters of any terrain features. It is also indirectly influence the hydrological
295 status of the basin. The quantitative morphometric evaluation has an intense utility to watershed
296 delineation, water and soil conservation and their management for future sustainability. The
297 morphometric analysis of the Yalamlam basin shows that the watershed has narrow, elongated
298 shape and very high mountainous relief. The planning for runoff and artificial recharge of the area
299 has been selected based on small-scale topographical maps and low relief (gentle slope) in the



300 lower area of the basin. Also drainage morphometric makes a positive role through GIS and remote
301 sensing techniques by selecting artificial recharge sites and the creation of demand storage point
302 in the mountainous region with the basin. In addition, if the morphometric information is integrated
303 with other hydrological parameter of the river basin, the strategy for water harvesting and
304 recharging measures gives a better plan for groundwater management and development for the
305 future.

306 The drainage pattern of the basin is sub dendritic and radial in nature. The pattern was affected by
307 more or less heterogeneous structural and lithological characteristics. In addition, high drainage
308 density is observed all over watershed along with very high relief and impermeable subsoils and
309 land rock substratum, mountainous terrain slope. On the other hand, lower riparian areas are low
310 drainage density, which are favorable for the identification of water storage areas and ground water
311 potential zones. However, slope plays a significant role in determining the relation between
312 infiltration rate and runoff velocity where infiltration rate is inversely controlled by regional slope.
313 So all evaluated parameters are more important to the analysis of future water availability of the
314 study region.

315 Results obtained from pervious scholarly work of Şen, (1995) pointed out that the average
316 transmissivity values calculated within the study area range from 91 to 147m²/day. While the the
317 transmissivity values increase sharply in the downstream area to range between 267 and 731
318 m²/day (average 500 m²/day). Such findings support the hypothesis that the aquifer is of high
319 potential therein. On the other hand, the hydraulic conductivity values calculated for Yalamlam
320 basin attain a high hydraulic conductivity (16 m/day) due to more permeable alluvial deposits (Sen,
321 1995, Elhag and Bahrawi 2014 b,c).



322 **5. Conclusions:**

323 The evaluation of hydrological characteristics of the Yalamlam watershed confirms that the area
324 is having high relief and the shape is elongated in nature. The stream network of the watershed is
325 basically dendritic type in lower portion which indicates the lack of structural influences and the
326 homogeneity of textural characteristics, but the upper portion of the watershed highly influenced
327 by tectonic and structural activity due to the parallel pattern of the drainage network. The drainage
328 characteristics of the basin help to understand the different kind of terrain parameters, i.e, runoff,
329 infiltration capacity and nature of the bedrock etc. The drainage density and frequency of the
330 drainage basin is low that indicates the high permeability rate and well-drained capacity of the sub
331 surface formation. All kinds of basic and derived parameters reveal an important the water
332 recharge areas and measures can be undertaken for the soil conservation structures and water
333 resource management. Therefore, watershed analysis using remote sensing data, GDEM data and
334 GIS techniques has an efficient, precise tool for the understanding of any terrain attributes such as
335 surface runoff, nature of bedrock, and infiltration capacity helps to better understanding of
336 drainage evolution and management of ground water potential and status of landform and their
337 characteristics for watershed management and planning. The study will be useful for water as well
338 as natural resource management of any terrain at the watershed level. For sustainable water
339 resource management and watershed development decision makers and planners can be used these
340 kinds of hydrological analysis.

341 The thickness of the saturated zone within the aquifer varies from less than 1 m upstream of
342 Yalamlam to about 30 m in the Sa'diyah area. The aquifer is generally unconfined, especially in
343 the upper parts of the wadi. Semi-confining conditions may exist in the lower parts where layers



344 of clay exist. There are about 31 wells in the basin of Wadi Yalamlam, out of which, 23 are hand-
345 dug wells and the others are drilled.

346 **Acknowledgement**

347 This article was funded by the Deanship of Scientific Research (DSR) at King Abdulaziz
348 University, Jeddah. The authors, therefore, acknowledged with thanks DSR for technical and
349 financial support.

350

351 **References**

352 Bahrawi, J. A., Elhag, M., Aldhebiani, A. Y., Galal, H. K., Hegazy, A. K. and Alghailani, E.
353 (2016). Soil Erosion Estimation Using Remote Sensing techniques in Wadi Yalamlam
354 basin, Saudi Arabia. *Advances in Materials Science and Engineering*,
355 DOI.org/10.1155/2016/9585962.

356 Drouineau, G. (1942). Dosage rapid du calcire actif du sol. Nouvelles donnes sur lareportation de
357 la nature des fractions calcaires. *Annual Agronomy*, 12: 411 - 450.

358 Elhag, M. (2014). Remotely sensed vegetation indices and spatial decision support system for
359 better water consumption Regime in Nile Delta. A case study for rice cultivation suitability
360 map. *Life Science Journal*, 11(1): 201-209.

361 Elhag, M. (2015). Characterization of a Typical Mediterranean Watershed Using Remote Sensing
362 Techniques and GIS Tools. *Hydrology: Current Research*, 6(1): 197-204.

363 Elhag, M. (2016). Evaluation of Different Soil Salinity Mapping Using Remote Sensing
364 Techniques in Arid Ecosystems, Saudi Arabia. *Journal of Sensors*, 2016: 96175-96175.

365 Elhag, M. and Bahrawi, J. (2014a). Potential Rainwater Harvesting Improvement Using Advanced
366 Remote Sensing Applications. *The Scientific World Journal*, DOI: 10.1155/2014/806959.



- 367 Elhag, M. and Bahrawi, J. (2014b). Conservational Use of Remote Sensing Techniques for a
368 Novel Rainwater Harvesting in Arid Environment. *Environmental Earth Sciences*, 72(12):
369 4995-5005.
- 370 Elhag, M. and Bahrawi, J. (2014c). Potential Rainwater Harvesting Improvement Using Advanced
371 Remote Sensing Applications. *The Scientific World Journal*, DOI: 10.1155/2014/806959.
- 372 Elhag, M. and Bahrawi, J. (2017). Realization of Daily Evapotranspiration in Arid Ecosystems
373 Based on Remote Sensing Techniques. *Geoscientific Instrumentation, Methods and Data*
374 *Systems*, 6: 1-10.
- 375 Elhag, M., Psilovikos, A. and Sakellariou, M. (2013). Detection of Land Cover Changes for Water
376 Recourses Management Using Remote Sensing Data over the Nile Delta Region.
377 *Environment, Development and Sustainability*, 15(5): 1189-1204.
- 378 Farr, T. G. and Kobrick, M. (2000). Shuttle radar topography mission produces a wealth of data.
379 *American Geophysical Union*, 81: 583–585.
- 380 Gotway, C. A., Ferguson, R. B., Hergert G. W. and Peterson, T. A. (1996). Comparison of kriging
381 and inverse distance methods for mapping soil parameters. *Soil Science Society of America*
382 *Journal*, 60: 1237-1247.
- 383 Grohmann, C. H., Riccomini, C. and Alves, F. M. (2007). SRTM-based morphotectonic analysis
384 of the Pocos de Caldas alkaline Massif, southeastern Brazil. *Computers and Geosciences*.
385 33: 10–19.
- 386 Hadley, R. F. and Schumn, S. A. (1961). Sediment sources and drainage basin characteristics in
387 the upper Cheyenn River Basin. *US Geological Survey. Water supply paper*, 1531-B: 137-
388 97.
- 389 Horton, R. E. (1945). Erosional development of streams and their drainage basins; hydrophysical
390 approach to quantitative morphology. *U.S. Geological Survey Professional*, p.282A.
- 391 Horton, R.E. (1932). Drainage basin characteristics. *Trans. Amer. Geophys. Union* 13, 350–361.



- 392 Johnson, L. W. and Riess, R. D. (1982). Numerical Analysis, 2nd ed. (Reading, MA:
393 AddisonWesley), Chapter, 1.3.
- 394 Leenaers, H., Okx, J. P. and Burrough, P. A. (1990). Employing elevation data for efficient
395 mapping of soil pollution on floodplain. *Soil Use and Management*, 6: 105-113.
- 396 Magesh, N., Chandrasekar, N. and Soundranayagam, J. (2011). Morphometric evaluation of
397 Papanasam and Manimuthar watersheds, parts of Western Ghats, Tirunelveli district,
398 Tamil Nadu, India: a GIS approach. *Environmental Earth Sciences*, 64: 373–381.
- 399 McLean, E. O. (1982). Soil pH and lime requirement. p. 199 - 224, In A. L. Page (ed.), *Methods*
400 *of soil analysis, Part 2: chemical and microbiological properties*. American Society of
401 *Agronomy*, Madison, WI, USA.
- 402 Miller, V. C. (1953). A Quantitative Geomorphologic Study of Drainage Basin Characteristics in
403 the Clinch Mountain Area, Virginia and Tennessee, Project NR 389042, Tech Rept 3.
404 Columbia University Department of Geology, ONR Geography Branch, New York.
- 405 Mueller, T. G., Pusuluri, N. B., Mathias, K. K., Cornelius, P. L., Barnhisel, R. I. and Shearer, S.
406 A. (2004). Map Quality for Ordinary Kriging and Inverse Distance Weighted Interpolation.
407 *Soil Science Society of America Journal*, 68: 2042-2047.
- 408 Panhalkar, S. S. (2014). Hydrological modeling using SWAT model and geoinformatic techniques.
409 *Egypt. The Egyptian Journal of Remote Sensing and Space Science*, 17(2): 197–207.
- 410 Pankaj, A. and Kumar, P. (2009). GIS based morphometric analysis of five major sub-watershed
411 of Song River, Dehradun district, Uttarakhand with special reference to landslide
412 incidences. *Journal of the Indian Society of Remote Sensing*, 37: 157–166.
- 413 Psilovikos, A. and Elhag, M. (2013). Forecasting of Remotely Sensed Daily Evapotranspiration
414 Data over Nile Delta Region, Egypt, *Water Resources Management*, 27(12): 4115-4130.
- 415 Richards, L. A. (1954). Diagnosis and improvement of saline and alkali soils. *USDA Agric.*
416 *Handbook 60*. Washington, D. C.



- 417 Schloeder, C. A., Zimmerman, N. E. and Jacobs, M. J. (2001). Comparison of methods for
418 interpolating soil properties using limited data. *Soil Science Society of America Journal*,
419 65: 470-479.
- 420 Schumm, S. A. (1956). Evolution of drainage systems and slopes in badlands at Perth Amboy,
421 New Jersey. *National Geological Society of America Bulletin*, 67: 597-646.
- 422 Schumm, S. A. (1963). Sinuosity of alluvial rivers in the Great Plains. *Bull. Geol. Soc. Am.* 74,
423 1089–1100.
- 424 Sen, Z. (1995). *Wadi Hydrology*. CRC Press, Taylor and Francis, New York.
- 425 Smith, K. G. (1950). Standards for grading texture of erosional topography. *American Journal of*
426 *Science*, 248: 655-668.
- 427 Sreedevi, P. D., Sreekanth, P. D., Khan, H. H. and Ahmed, S. (2013). Drainage morphometry and
428 its influence on hydrology in a semi-arid region: using SRTM data and GIS. *Environmental*
429 *Earth Science*, 70 (2): 839–848.
- 430 Stoer, J. and Bulirsch, R. (1980). *Introduction to Numerical Analysis* (New York: Springer-
431 Verlag), Chapter 2.
- 432 Strahler, A. N. (1964). Quantitative Geomorphology of drainage basins and channel networks.
433 *Handbook of Applied Hydrology*; edited by V.T Chow (Newyork; Mc Graw hill) Section
434 4-11.
- 435 Strahler, A.N., (1957). Quantitative analysis of watershed geomorphology. *Trans. Am. Geophys.*
436 *Union* 38, 913–920.
- 437 Walsh, L. M. and Beaton, J. D. (1973). *Soil testing and plant analysis*. Soil Science Society of
438 America, Madison. WI, USA.
- 439 Weibel, R. (1997). A Typology of Constraints to Line Simplification. In: Kraak, M. J. and
440 Molenaar, M. (eds.): *Advances in GIS Research II* (7th International Symposium on Spatial
441 Data Handling). London: Taylor and Francis, pp. 533-546.



- 442 Weller, U., Zipprich, M., Sommer, M., zu Castell, W. and Wehrhan, M. (2007). Mapping clay
443 content across boundaries at the landscape scale with electromagnetic induction. Soil
444 Science Society of America Journal, 71:1740–1747.
- 445 Westerman, R. L. (1990). Soil testing and plant analysis. 3rd ed. Soil Science Society of America,
446 Madison, WI, USA.
- 447 Wollenhaupt, N. C., Wolkowski, R. P. and Clayton, M. K. (1994). Mapping soil test phosphorus
448 and potassium for variable-rate fertilizer application. Journal of Production Agriculture,
449 7(4):441-448.
- 450 YanYun, N. I. A. N., Xin, L. I., Jian, Z. H. O. U., and XiaoLi. H. U. (2014). Impact of land use
451 change on water resource allocation in the middle reaches of the Heihe River Basin in
452 northwestern China. Journal of Arid Land, 6 (3), 273–286.
- 453
- 454
- 455
- 456